Spline spaces over rectangular meshes with arbitrary topologies and its application to the Grad-Shafranov equation

Meng Wu, Bernard Mourrain, André Galligo, Boniface Nkonga

Spline spaces over rectangular meshes with arbitrary topologies and its application to the Grad-Shafranov equation

Meng Wu[a,c,*], Bernard Mourrain[a], André Galligo[b], Boniface Nkonga[b]

[a] *Galaad2, Inria, Sophia Antipolis, France*
[b] *Lab. J. A. Dieudonné, University of Nice, Nice, France*
[c] *School of Mathematics, Hefei University of Technology, P. R. China.*

Abstract

Motivated by the magneto hydrodynamic (MHD) simulation for tokamaks with an isoparametric finite element method or isogeometric analysis, we present a new type of spline space defined over a rectangular mesh with arbitrary topology. A set of bases called Hermite bases is constructed and applied to solving the Grad-Shafranov equation which is the equilibrium in the resistive MHD model. H^1 integrability assumption is used for designing parameterizations of the examples. Because the Grad-Shafranov equation is the second order PDE and there are isolated singularities of the parameterizations generally. To validate the continuity of the numerical solution of the Grad-Shafranov equation and its gradients on the physical domain, the errors between the exact solution and the numerical solution are compared with the L^2-norm and H^1-norm. The optimal convergence rates are reached.

Keywords: Spline, Arbitrary topology meshes, Dimension and basis, the Grad-Shafranov equation, Isoparametric finite elements, Isogeometric analysis

1. Introduction

The finite element method (FEM) is a powerful tool that is often used to derive accurate and robust scheme for the approximation of the solution of PDEs. We are concerned with MHD equations applied to the edge plasma of fusion devices as tokamaks. In this context of strongly magnetized plasma, the finite element formulation faces some difficulties such as the divergence-free constraint and the high anisotropy of transport processes. For applications to tokamaks, the divergence-free constraint is enforced by the introduction of the potential vector: the magnetic field becomes the

*Corresponding author at: Galaad2, INRIA Sophia-Antipolis, 2004 Route des Lucioles, 06902 Cedex, France; School of Mathematics, Hefei University of Technology, No. 193, Tunxi Road, Hefei, Anhui Prov., 230009, P. R. China.

Email addresses: meng.wu@hfut.edu.cn, wumeng@mail.ustc.edu.cn (Meng Wu), Bernard.Mourrain@inria.fr (Bernard Mourrain), andre.galligo@unice.fr (André Galligo), boniface.nkonga@unice.fr (Boniface Nkonga)

rotational of this vector. For the resistive MHD model, this leads to a system of partial differential equations of order greater than two. In this paper, the Grad-Shafranov equation is considered, which is the equilibrium in the resistive MHD model. The weak formulations require test functions that are continuously differentiable (C^1), but because of the lack of smoothness (gradients are discontinuous), classical Lagrange finite elements cannot be directly applied.

On the other hand, higher anisotropies suggest the use of meshes aligned with the principal directions of the transport processes [1]. These directions are prescribed by the magnetic flux surfaces, and in this first approach, we assume that we are close to a given equilibrium so that the alignment can be achieved at the initial step. Unfortunately, for high-confinement tokamaks, there is a saddle point, and the associated magnetic flux is singular. In this context, quadrilateral (2D) and hexahedral (3D) meshes are the most convenient for alignment and lead to a reduction in the approximation error. The construction of high-quality block structured meshes is a challenging issue when considering complex geometries, even if isoparametric finite elements [2] or isogeometric analysis [3] can help to fit on physically curved boundaries. For example, in our target application, to align the principal directions of the transport processes, a structured mesh is involved, as shown on the left side of Figure 2.

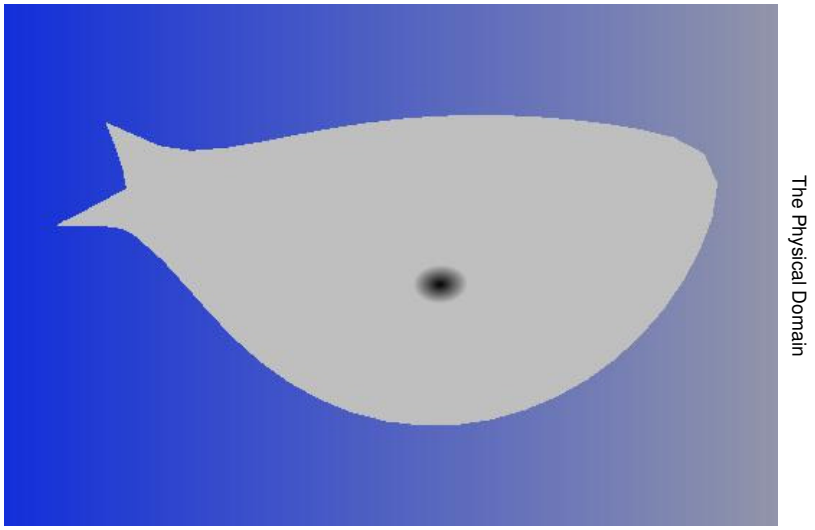

Figure 1: Physical domain of the target application

Although tensor product B-splines [4], hierarchical B-splines [5],[6],[7], LR-splines [8] and T-splines [9] are often used as shape functions, they satisfy the regularity

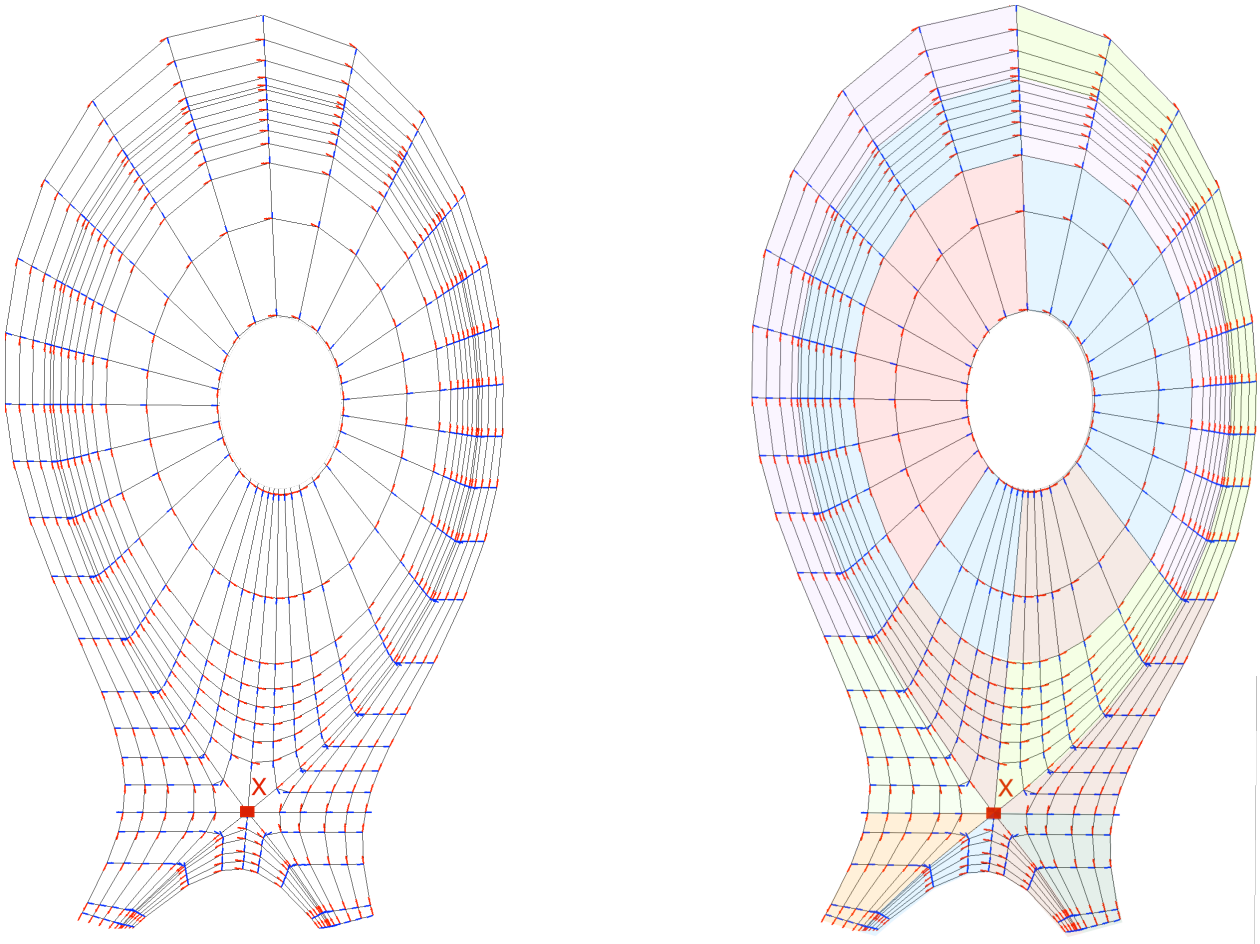

Figure 2: The structured mesh of the target application and its block structured mesh

requirement but are associated with simpler topological structures than that needed for our target applications. For example, one of restrictions is that the physical domains should be homeomorphic to rectangles because all of these splines are defined over rectangular parameter domains. In other words, the structured mesh on the left side of Figure 2 has to be decomposed when these splines are treated as shape functions. On the right side of Figure 2, there is one method for decomposing this structured mesh.

Splines defined over a manifold or a mesh with arbitrary topology are one way to avoid decomposing the mesh if they are treated as shape functions. Splines defined over a manifold is based on the classical definition of a differential manifold, such as [10, 11, 12, 13]. Its local charts of the differential manifold are open sets, and the intersections between local charts are open sets. For splines defined on a mesh with arbitrary topology, such as [14]. Its local charts are rectangles called cells, and the intersections between two local charts form a corner point (vertex), a segment (edge) or an empty set. By generalising splines defined on a mesh with arbitrary topology in [14], a type of spline will be proposed in this paper. They can be treated as shape functions for solving PDEs with isoparametric finite elements or isogeometric analysis globally without decomposing the structured meshes.

Besides defining spline spaces over rectangular meshes with arbitrary topologies, the other main objective of this paper is to propose basis functions of this type of spline over meshes with arbitrary topology, which apply them to solve the Grad-Shafranov equation. In [15], isoparametric bicubic Hermite elements are used to solve the Grad-Shafranov equation over a physical domain with concentric-circle-like iso-curves. They introduced a polar-coordinate-like transformation to construct a global coordinate system to conserve the desirable properties of the classical cubic Hermite element [16]. With splines defined in this paper, a general physical domain with complex iso-curves can be described globally, not only for a physical domain with concentric-circle-like iso-curves. For the continuity of the numerical solution and its gradients, the errors with L^2-norm and H^1-norm are presented as [1].

Concretely, from Section 2 to Section 4, we focus on defining this type of spline spaces and constructing the basis functions, called Hermite bases in this paper. Section 2 presents the definition of meshes with arbitrary topologies in the parametric plane, called parametric meshes, following [14]. Then, we define spline spaces over parametric meshes. Section 3 concentrates on the solution of the basic problems for a spline space over a parametric mesh with bi-degree $(3, 3)$ and C^1 regularity, in other words, C^1 global functions over a parametric mesh. We provide formulas for the dimensions and describe Hermite bases that will be used in Section 4. In Section 4, the convergence behavior for solving the Grad-Shafranov equation is analyzed. Before solving the Grad-Shafranov equation, in Section 4.1, the property of parameterizations is discussed. In Section 4.2, we analyze the approximation error of these splines and solve the Grad-Shafranov equation over physical domains with meshes that have arbitrary topologies. To validate the continuity of the solution of the Grad-Shafranov equation and its gradient, the errors are analyzed with L^2-norm and H^1-norm respectively. The last section proposes a conclusion of our work and directions for future works.

2. Meshes in the parametric plane and spline spaces

In this section, the fundamental definitions of this paper will be presented. First, in Section 2.1, the concept of parametric meshes is given. Its definition includes an equivalence relation, which allows to addressing more general topologies. Then the definition of spline spaces over a parametric mesh is introduced in Section 2.2.

2.1. Parametric meshes

In this section, we introduce our concept of a parametric mesh, which generalizes the notion of a mesh in the parametric space, considered, e.g., in [17], [8] and [14]. Concretely, in Section 2.1.1, the definition of parametric meshes is given. Then, some concepts are introduced in Section 2.1.2, such as local frames, hanging vertices, basis vertices and composite edges of a parametric mesh, which will be used in Sections 2.2 and 3. Moreover, the local refinement of meshes is necessary for adaptive finite element method. Section 2.1.3 will introduce how to perform a local refinement of a parametric mesh. In the process, the definition of hierarchical parametric meshes is presented based on a local refinement process.

2.1.1. Definition of Parametric Meshes

Notation 2.1. *The metric plane $\mathbb{R}^2$ equipped with coordinates (s,t), will be called the $(s,t)-$plane. A cell is a rectangle of $\mathbb{R}^2$. We will use the letter C with indices to denote cells. The boundary of a cell is decomposed into a finite set of segments (at least 4 but maybe more), called the edges of the cell. We will use the letter e with indices to denote edges. The end points of these edges are called the vertices of the cell. We will use the letters v or w with indices to denote vertices.*

We will consider an equivalence relation on the vertices (resp. edges) of a union of cells. Before providing a formal definition of our concept, let us illustrate it with a simple example to show a parametric mesh with arbitrary topology.

Example 2.1 (A parametric mesh with arbitrary topology). *The left mesh of Figure 3 shows a parametric mesh $\mathscr{M}$. Its equivalent vertices have been marked with the same vertex labels and the edges between equivalent vertices are equivalent.*

The topological structure of $\mathscr{M}$ is the same as the topology of a "usual" mesh, shown on the right side of Figure 3. From this example, a parametric mesh allows extraordinary vertices, whose valences are not 4.

Now, the formal definition of a parametric mesh is presented.

Definition 2.1 (Parametric Mesh). *A parametric mesh $\mathscr{M}$ is given by a collection of cells denoted by $C_1, C_2, \cdots, C_N$, a subset $\mathscr{P}_F$ of $\mathrm{I} = \{\{i,j\} : i,j \in \{1,2,\cdots,N\} \text{ and } i \neq j\}$, a collection of transition maps indexed by $\mathscr{P}_F$, and an equivalence relation " $\sim$ " on the edges and vertices of the cells, satisfying the following properties.*

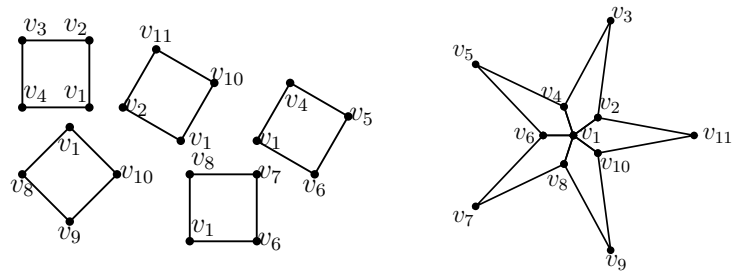

Figure 3: A parametric mesh $\mathscr{M}$ with 5 cells (left) and a "usual" mesh with the same topology of $\mathscr{M}$

1. *For each pair $(i,j) \in \mathscr{P}_F$, there exists a pair of transition maps:*
   - $\phi_{i,j} : C_i \to \mathbb{R}^2$,
   - $\phi_{j,i} : C_j \to \mathbb{R}^2$

   and a pair of edges $e_{i,j}$ of C_i and $e_{j,i}$ of C_j such that
   - $\phi_{i,j}(C_i) \cap C_j = e_{j,i}$,
   - $\phi_{j,i}(C_j) \cap C_i = e_{i,j}$,
   - $\phi_{i,j}|_{e_{i,j}} : e_{i,j} \longrightarrow e_{j,i}$, $\phi_{j,i}|_{e_{j,i}} : e_{j,i} \longrightarrow e_{i,j}$ *are diffeomorphisms and* $(\phi_{i,j}|_{e_{i,j}})^{-1} = \phi_{j,i}|_{e_{j,i}}$.

   Then, $e_{i,j} \sim e_{j,i}$.

   Moreover, for any two vertices v of $e_{i,j}$ and w of $e_{j,i}$, if $\phi_{i,j}(v) = w$ then $v \sim w$.
2. *For any edge e of C_i $(i = 1, 2, \cdots, n)$, the number of edges that are equivalent to e by "$\sim$" is no more than 2.*

Definition 2.2 (Interior vs Boundary, degree). *The equivalence class of edges and vertices of C_i are called $\mathscr{M}$'s edges and vertices. If an edge equivalence class has two elements, then it is called an interior edge of $\mathscr{M}$; otherwise it is called a boundary edge. If a vertex is on a boundary edge, then it is called a boundary vertex; otherwise, it is called an interior vertex. The degree $deg(v)$ of an equivalence class of vertices v is the number of distinct equivalence classes of edges e containing v.*

Example 2.2. *In Example 2.1, note that, e.g., v_6v_7 is a boundary edge, while v_1v_2 and v_1v_6 are interior edges (because they are shared by two cells). We have $deg(v_1) = 5$, $deg(v_2) = 3$ and $deg(v_3) = 2$.*

Remark 2.2 (Restrictions).

- *A parametric mesh can also describe a non-orientable surface, such as the Moebius strip. However, in this article, we will restrict ourselves to the case where $\mathscr{M}$ is orientable. Furthermore, we suppose that any edge (resp. vertex) of a cell is not equivalent to another edge (resp. vertex) of the same cell.*
- *In this paper, we will also only consider parametric meshes with transition maps that are rigid transformations.*

2.1.2. Local frames, hanging vertices, basis vertices and composite edges of a parametric mesh

Let $\mathscr{M}$ be a parametric mesh and denote its cells as $C_1, C_2, \cdots, C_N$. For each cell C_i, $i = 1 \ldots N$, we define a local frame by two unit vectors $\mathscr{F}_i := (\mathbf{s}_i, \mathbf{t}_i)$ that parallel each of the two directions of the edges of C_i (and that agrees with the metric of the (s,t)–plane). This is illustrated in Figure 4.

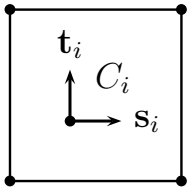

Figure 4: A local frame of C_i

Now consider two adjacent cells C_1 and C_2 of $\mathscr{M}$, (i.e., that share a common edge).

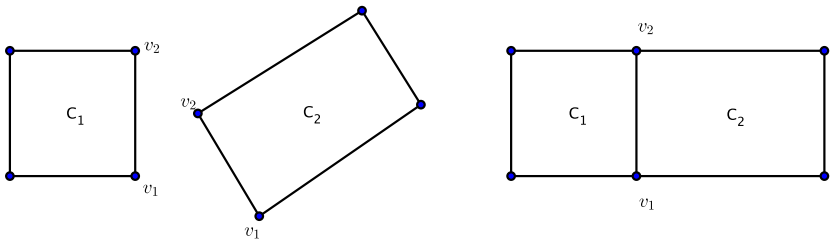

Figure 5: Transition maps

They can be moved together by the transition map, which is a rigid transformation. This is illustrated in Figure 5. By this way, $\mathscr{M}$ becomes another parameter mesh $\mathscr{M}'$ with identity transition maps between two adjacent cells, where $\mathscr{M}'$ is called an equivalent parametric mesh of $\mathscr{M}$.

Example 2.3 (A T-mesh). *A planar T-mesh, as defined in [17], can be represented by a parametric mesh such as the right side of Figure 6, where all of the transition maps are identity maps.*

In the left side of Figure 6 there is another parametric mesh with all of the transition maps, which are rigid transformations. The T-mesh in the right side of Figure 6 is an equivalent parametric mesh of the parametric mesh in the left side of Figure 6.

Definition 2.3. *Here, we present the definitions of a hanging vertex, basis vertex and composite edge.*

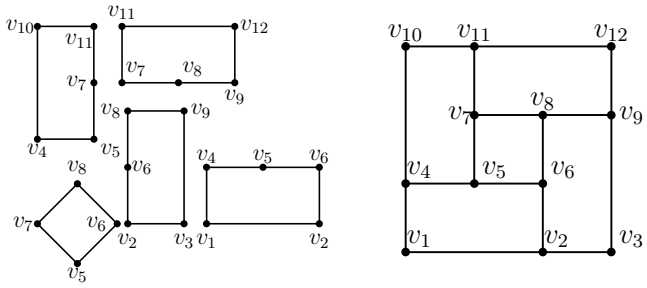

Figure 6: A parametric mesh with rigid transformations and its equivalent parametric mesh with identity transition maps

- *An interior vertex v of $\mathscr{M}$ is called a hanging vertex if there is a cell C such that v is on an edge of C and it is not a corner point of C.*
- *A vertex of $\mathscr{M}$ that is not a hanging vertex is called a basis vertex.*
- *A composite edge of $\mathscr{M}$ is the longest possible "line segment" that consists of several interior edges, and each non-end vertex of this "line segment" is a hanging vertex of $\mathscr{M}$, where if two edges locate on the same line or not, this point is determined by their positions in $\mathscr{M}$'s equivalent parametric mesh.*

Example 2.4. *In the left side of Figures 6, the vertices v_5,v_7,v_6 and v_8 are hanging vertices, v_5v_7 is an interior edge, and v_5v_{11} is a composite edge that includes two edges v_5v_7 and v_7v_{11}. Because v_5v_{11} lies on the same line of its equivalent parametric mesh (T-mesh), shown in the right side of Figure 6, it satisfies the definition of "a composite edge".*

Remark 2.3. *If $\mathscr{M}$ has no hanging vertices and all of its cells are unit squares, it is* **a spline domain**, *as defined in [14].*

2.1.3. Local Refinement and Hierarchical parametric meshes

In adaptive finite element analysis, refinement is an important operation. Traditionally, one distinguishes between two types of refinement: h-refinement and p-refinement. The first one, also called h-adaptivity, amounts to splitting elements in space while keeping their polynomial degree fixed, whereas p-adaptivity amounts to increasing the polynomial degrees.

Hereafter, a simple scheme of the local h-refinement of $\mathscr{M}$ is presented. The refinement does not change the topology of $\mathscr{M}$.

Definition 2.4 (Local Refinement Rule). *Let $\mathscr{M}$ be a parametric mesh. A refined parametric mesh $\mathscr{M}'$ is obtained by splitting some of the cells of $\mathscr{M}$ along lines parallel to one of the edges of these cells. The transition maps of $\mathscr{M}'$ are defined as follows.*

- *Given two cells C_i and C_j of $\mathscr{M}$ with an adjacent edge $e_{i,j} \sim e_{j,i}$ which is split, for any cells $C'_{i'} \subset C_i$, $C'_{j'} \subset C_j$ of $\mathscr{M}'$ with a common sub-edge of $e_{i,j} \sim e_{j,i}$, the transition map between $C'_{i'}$ and $C'_{j'}$ is the restriction respectively to $C'_{i'}$ and $C'_{j'}$ of the transition maps $\phi_{i,j} : C_i \longrightarrow \mathbb{R}^2$ and $\phi_{j,i} : C_j \longrightarrow \mathbb{R}^2$.*
- *For a cell C of $\mathscr{M}$ split into sub-cells C'_1, C'_2 of $\mathscr{M}'$ along an edge e', the transition map across e' is the identity.*

This refinement construction can be iterated. Notice that the refinements create additional hanging vertices.

Definition 2.5 (Hierarchical parametric mesh). *A hierarchical parametric mesh $\mathscr{M}$ is a mesh obtained by the iterated refinement of an initial parametric mesh, where we will also assume that the initial mesh has no hanging vertex.*

If the initial mesh is just a cell, $\mathscr{M}$ is a hierarchical T-subdivision, as described in [25].

2.2. Spline spaces over a parametric mesh

In this section, based on the definition of a parametric mesh in Section 2.1, we define the spline space over a parametric mesh in Section 2.2.1. Formally, this definition depends on the choice of local frames. In Section 2.2.2, the local frame independency will be checked. After that, in Section 2.2.3, the nesting property of spline spaces is presented by the local refinement of parametric meshes. It is necessary to apply to adaptive finite element analysis.

2.2.1. Definition of spline spaces over a parametric mesh

Definition 2.6 (Spline over $\mathscr{M}$). *A spline f of bi-degree (d, d) and C^r regularity over $\mathscr{M}$ with the local frame set $\mathscr{F} = \{\mathscr{F}_i\}$ is given by a collection of polynomials f_i satisfying*
1. $f_i(s_i, t_i) := f|_{C_i} \in \mathbb{R}_{d,d}[s_i, t_i]$, $i = 1 \dots N$, where (s_i, t_i) is the coordinates associated with the given local frame $\mathscr{F}_i$ of C_i;
2. If $v_{i,j} \sim v_{j,i}$ is a (class) of vertex common to cells C_i and C_j of $\mathscr{M}$, then

$$f_i(v_{i,j}) = f_j(v_{j,i}).$$

3. If $e_{i,j} \sim e_{j,i}$ is a (class) of edge common to cells C_i and C_j of $\mathscr{M}$, then $f_i(s_i, t_i)$ and $f_j(s_j, t_j)$ are "C^r across the edge"(we will also say that they have a C^r fit).

More precisely, let $\phi_{i,j}, \phi_{j,i}$ be the transition maps between C_i and C_j, such that $\phi_{i,j}(e_{i,j}) = e_{j,i}$; denote as $\mathbf{n}_{i,j}$ and $\mathbf{n}_{j,i}$ unit vectors of the metric $(s,t)-$plane, perpendicular, respectively, to $e_{i,j}$ and $e_{j,i}$. Then, we must have

$$D^k_{\mathbf{n}_{i,j}}(f_j \circ \phi^{-1}_{j,i})|_{e_{i,j}} = D^k_{\mathbf{n}_{i,j}} f_i|_{e_{i,j}} \tag{1}$$

$$D^k_{\mathbf{n}_{j,i}}(f_i \circ \phi^{-1}_{i,j})|_{e_{j,i}} = D^k_{\mathbf{n}_{j,i}} f_j|_{e_{j,i}} \tag{2}$$

for $k = 0, 1, 2, \cdots, r$.

Remark 2.4. *If $\forall \phi_{i,j}, \phi_{j,i}$ are rigid transformations and $\forall C_i$ are unit squares, then the splines defined here are C^r-splines in [14].*

Notation 2.5. *We denote by $\mathbf{S}(d, r; \mathscr{M})$ the set of splines defined in Definition 2.6. We call it a spline space over $\mathscr{M}$.*

We have:

- By linearity of directional derivatives, $\mathbf{S}(d, r; \mathscr{M})$ is a vector space;
- It is finite dimensional;
- $1 \in \mathbf{S}(d, r; \mathscr{M})$.

Remark 2.6. *Note that since we assumed that the transition maps are rigid transformations, conditions* (1) *and* (2) *are equivalent.*

2.2.2. Spline space and local frames

Let us discuss the dependency of the spline space $\mathscr{M}$ on the choice of local frames $\mathscr{F}_i$ for the cells C_i.

Considering another local frame $\mathscr{F}_i'$, there exists a set of orthogonal transformations $\mathbf{O} = \{\mathbf{O}_i\}$ such that

$$\mathscr{F}_i = \mathbf{O}_i \mathscr{F}_i', i = 1 \dots N.$$

By the action of $\mathbf{O}_i$, any polynomial in the coordinates of $\mathscr{F}_i$ becomes a polynomial in the coordinates of $\mathscr{F}_i'$ of the same degree. Moreover, the other two items in Definition 2.6, evaluation at a vertex and regularity, are conserved when expressed in the other frame. This proves the following theorem.

Theorem 2.7 ($\mathscr{F}$ Independency). *Let $\mathscr{F}$ and $\mathscr{F}'$ be two local frames of $\mathscr{M}$. Then, for each cell C_i, $i = 1 \dots N$, of $\mathscr{M}$, there exists an orthogonal transformation $\mathbf{O}_i$ sending $\mathscr{F}_i'$ to $\mathscr{F}_i$, i. e., $\mathscr{F}_i = \mathbf{O}_i \mathscr{F}_i'$. If $f \in \mathbf{S}(d, r; \langle \mathscr{M}, \mathscr{F} \rangle)$, so that*

$$f \circ \mathbf{O} \in \mathbf{S}(d, r; \langle \mathscr{M}, \mathscr{F}' \rangle),$$

where $\mathbf{O}|_{\mathscr{F}_i} = \mathbf{O}_i$, $f \circ \mathbf{O}|_{C_i} = f(\mathbf{O}_i(s_i', t_i'))$, where $\mathbf{S}(d, r; \langle \mathscr{M}, \mathscr{F} \rangle)$ is a spline space over $\mathscr{M}$ with the local frames $\mathscr{F}$. Its bi-degree is (d, d) and, it has C^r regularity.

Thus, up to a set of orthogonal transformations, splines over $\mathscr{M}$ are independent of the choice of $\mathscr{F}$.

2.2.3. Local refinement and spline spaces

Let $\mathscr{M}'$ be a parametric mesh obtained by refining some cells of $\mathscr{M}$. Then, a spline function in $\mathbf{S}(d, r; \mathscr{M})$ is a spline function defined over the refined mesh $\mathscr{M}'$, owing to the local refinement rule in Definition 2.4.

Thus, we have the nesting property:

$$\mathbf{S}(d, r; \mathscr{M}) \subseteq \mathbf{S}(d, r; \mathscr{M}').$$

In particular, we still have

$$1 \in \mathbf{S}(d, r; \mathscr{M}').$$

3. Bicubic spline spaces over a parametric mesh

In this section, bicubic spline spaces over a parametric mesh will be considered and used for applications in Section 4. The main results in this section present the dimension formula and a set of bases, where Hermite data play a crucial role.

Let $\mathscr{M}$ be a hierarchical mesh. The bicubic spline spaces over $\mathscr{M}$ is $\mathbf{S}(3,1;\mathscr{M})$. Here, we organize this section as follows. In Section 3.1, the Hermite data of a bicubic spline over a parametric mesh are discussed. Based on the analysis of Section 3.1, in Section 3.2, the dimension formula of $\mathbf{S}(3,1;\mathscr{M})$ and a set of bases are presented.

3.1. Hermite data

In this section, a linear map $\mathscr{H}$ is introduced. By $\mathscr{H}$, a spline in $\mathbf{S}(3,1;\mathscr{M})$ is described by its Hermite data at each vertex of $\mathscr{M}$. Then, the constraints between its Hermite data are given, such that the constraints across a common edge (Section 3.1.1) become the constraints of the Hermite data at a basis vertex and hanging vertex (Section 3.1.2). By these constraints, $\mathscr{H}$ is reduced to a new injective map $\widetilde{\mathscr{H}}$.

We first illustrate the Hermite data construction on a single square. Let Q be the square in the parametric (s,t)-plane with vertices $v_1 := [0,0]$, $v_2 := [0,1]$, $v_3 := [1,0]$, and $v_4 := [1,1]$. The vector space E of polynomials of bidegree $(3,3)$ on Q has dimension 16 and a basis of E is formed by the two by two products of Bernstein polynomials $B_i^3(s)$ and $B_j^3(t)$ for $0 \le i,j \le 3$.

We set

$$H^{v_\ell}_{(s,t)}(f) = (f(v_\ell), \frac{\partial f}{\partial s}(v_\ell), \frac{\partial f}{\partial t}(v_\ell), \frac{\partial^2 f}{\partial s \partial t}(v_\ell))$$

for $1 \le \ell \le 4$.

The 4 Hermite data $H^{v_\ell}_{(s_i,t_i)}(f)$ at each of the 4 vertices form 16 real numbers naturally associated with an element f of E.

Lemma 3.1. *The linear map $E \longrightarrow \mathbb{R}^{16}$ defined by the Hermite data at the 4 vertices of Q is an isomorphism.*

Proof. It suffices to check the non vanishing of the determinant of the corresponding matrix on the basis $B_i^3(s)B_j^3(t)$, $0 \le i,j \le 3$. □

Notice that $H^{v_\ell}(f)$ depends only on the four Bernstein coefficients that are near v_ℓ as in the B-net method described in [17]. By this correspondence, the dimension formula and basis construction of $\mathbf{S}(3,1;\mathscr{M})$ are discussed by generalizing the B-net method in [17].

Let $\mathscr{M}$'s cells be $C_1,\ldots,C_N$. We extend the definition of the Hermite data to the spline space $\mathbf{S}(3,1;\mathscr{M})$ and via the following map:

$$\begin{aligned} \mathscr{H} : \mathbf{S}(3,1;\mathscr{M}) &\rightarrow \mathbb{R}^{4N} \\ f &\mapsto (H^{v^i_\ell}_{(s_i,t_i)}(f_i))_{i=1,\ldots,N,\ell=1,\ldots,4} \end{aligned} \tag{3}$$

where $v^i_\ell, \ell = 1,\ldots,4$ are the 4 vertices of cell C_i and $H^{v^i_\ell}_{(s_i,t_i)}(f_i)$ are the Hermite data of f at v^i_ℓ.

Lemma 3.2. *The Hermite data map $\mathscr{H}$ defined in* (3) *is an injective linear map from* $\mathbf{S}(3,1;\mathscr{M})$ *to* $\mathbb{R}^{4N}$.

Proof. By construction, $\mathscr{H}$ is linear. To prove that it is injective, we note that if all Hermite data of a polynomial f_i at the vertices of a cell C_i are zero, then by Lemma 3.1, $f_i \equiv 0$. Thus, if $f \in \mathbf{S}(3,1;\mathscr{M})$ is such that $\mathscr{H}(f) = 0$ then $f = 0$. □

We now analyze different constraints applicable on the Hermite data at a vertex of $\mathscr{M}$.

3.1.1. Hermite data across a common edge

In this section, we describe a C^1 regularity condition across an edge in terms of Hermite data.

Lemma 3.3. *Let C_1, C_2 be two cells with the common edge $e_{1,2} = v_1v_2$. Assume that they share the same local frame $(\mathbf{s}, \mathbf{t})$ and the same parameters (s,t). Then $f_1(s,t)$ and $f_2(s,t)$ are C^1 across $e_{1,2}$ if and only if their Hermite data at v_1 and v_2 coincide:*

$$H^{v_\ell}_{(s,t)}(f_1) = H^{v_\ell}_{(s,t)}(f_2),\ l = 1, 2.$$

Proof. Suppose that the edge $e_{1,2}$ is along the t-direction (the other case can be treated symmetrically). Because $f_1(s,t)$ and $f_2(s,t)$ are polynomials of bi-degree $(3,3)$, if their Hermite data coincide at v_1 and v_2, then we have $f_1(s,t) = f_2(s,t)$ and $\partial_s f_1(s,t) = \partial_s f_2(s,t)$ along the edge $v_1v_2 = e_{1,2}$. In other words, the function defined by (f_1, f_2) is C^1 across the edge $e_{1,2}$

Conversely, if (f_1, f_2) is C^1 across the edge $e_{1,2}$, then their Hermite data at v_1 and v_2 must coincide. □

Assume now that C_1 and C_2 have different frames, denoted by $\mathscr{F}_1 = (\mathbf{s}_1, \mathbf{t}_1)^T$ and $\mathscr{F}_2 = (\mathbf{s}_2, \mathbf{t}_2)^T$. There must exist an orthogonal transformation $\mathbf{O}_{2,1}$, more precisely a rotation of angle $k\pi/2$ ($k \in \mathbb{Z}$), such that

$$\mathscr{F}_2 = \mathbf{O}_{2,1}\mathscr{F}_1. \tag{4}$$

The following lemma describes the relations between $H^{v_\ell}_{(s_1,t_1)}(f_1)$ and $H^{v_\ell}_{(s_2,t_2)}(f_2)$.

Lemma 3.4. *$f_1(s_1,t_1)$ and $f_2(s_2,t_2)$ have a C^1 fit if and only if*

$$H^{v_\ell}_{(s_2,t_2)}(f_2)^T = AH^{v_\ell}_{(s_1,t_1)}(f_1)^T, \tag{5}$$

where

$$A = \begin{pmatrix} 1 & 0 & 0 \\ 0 & \mathbf{O}_{2,1} & 0 \\ 0 & 0 & O_{11}O_{22} + O_{12}O_{21} \end{pmatrix} \tag{6}$$

and

$$\mathbf{O}_{2,1} = \begin{pmatrix} O_{11} & O_{12} \\ O_{21} & O_{22} \end{pmatrix}.$$

Proof. By Lemma 3.3, after applying the transition map, we have $H^{v_\ell}_{(s_1,t_1)}(f_1)^T = H^{v_\ell}_{(s_2,t_2)}(f_2)^T$. Thus, we just considered the Hermite data at v_ℓ of f_2 using different frames $\mathscr{F}_1, \mathscr{F}_2$. Based on the fact that $\mathbf{O}_{2,1}$ is an orthogonal rotation of angle $k\pi/2$, we explicitly computed matrix A and obtained formula (6). □

Remark 3.5. *Because* $\mathbf{O}_{2,1}$ *is a rotation of angle* $k\pi/2$*, we have* $O_{11}O_{22} + O_{12}O_{21} = (-1)^k$*; consequently* $\mathrm{rank}(A) = 4$*.*

This shows that the Hermite data at v_ℓ on C_2 is uniquely determined by the Hermite data at v_ℓ on C_1, via the linear invertible transformation A. In this case we will say that the Hermite data at v_ℓ on C_1 and C_2 are **compatible**.

3.1.2. Hermite data at a basis vertex of degree n and a hanging vertex

Let v be a basis vertex of $\mathscr{M}$ and n be the degree of v. This means that there are n cells $C_1, \ldots, C_n$ with v as one of their corner vertices. These cells form v's 1-neighborhood. Let us consider the behavior of $f \in \mathbf{S}(3, 1; \mathscr{M})$ at v.

We can assume that we have already sorted the 1-neighborhood of v such that two successive cells share a common edge of $\mathscr{M}$.

Given a local frame $\mathscr{F}_1 = (\mathbf{s}_1, \mathbf{t}_1)^T$ of C_1, the local frame $\mathscr{F}_k$ of C_k is defined as

$$\mathscr{F}_k = \mathbf{O}_{k,1}\mathscr{F}_1, \tag{7}$$

where

$$\mathbf{O}_{k,1} = \begin{pmatrix} \cos(-\pi(k-1)/2) & -\sin(-\pi(k-1)/2) \\ \sin(-\pi(k-1)/2) & \cos(-\pi(k-1)/2) \end{pmatrix}$$

According to C^1 continuity, the Hermite data at v of C_k is obtained by Eq. (4) and Eq. (5), i.e.,

$$H^v_{(s_k,t_k)}(f)^T = A_k H^v_{(s_1,t_1)}(f)^T, \tag{8}$$

where A_k is determined by $\mathbf{O}_{k,1}$, similarly to Eq. (5). Because v is a basis vertex, it can be a boundary vertex as well as an interior (not hanging) vertex. If v is a boundary vertex of $\mathscr{M}$, the Hermite data of $H^v_{(s_k,t_k)}(f)$ $(k > 1)$ are well determined when $H^v_{(s_1,t_1)}(f)$ is given because $\mathrm{rank}(A_k) = 4$.

If v is an interior vertex of $\mathscr{M}$, C_1 and C_n must stick together, i.e. share the same edge going clockwise. This gives rise to linear constraints that we now describe.

Proposition 3.6. *With the previous notations, if* v *is an interior basis vertex and* n *is its degree, we have*

1. *When* $n \mod 4 = 1$*, the Hermite data should satisfy*

$$H^v_{(s_1,t_1)}(f)^T = A_3 H^v_{(s_1,t_1)}(f)^T,$$

i.e.,

$$\begin{pmatrix} 0 & 0 & 0 & 0 \\ 0 & 1 & 1 & 0 \\ 0 & -1 & 1 & 0 \\ 0 & 0 & 0 & 2 \end{pmatrix} H^v_{(s_1,t_1)}(f)^T = 0$$

Then,

$$\frac{\partial f(v)}{\partial s_1} = 0, \frac{\partial f(v)}{\partial t_1} = 0, \frac{\partial^2 f(v)}{\partial s_1 \partial t_1} = 0;$$

2. *When* $n \mod 4 = 2$*, the Hermite data should satisfy*

$$H^v_{(s_1,t_1)}(f)^T = A_2 H^v_{(s_1,t_1)}(f)^T,$$

i.e.

$$\begin{pmatrix} 0 & 0 & 0 & 0 \\ 0 & 2 & 0 & 0 \\ 0 & 0 & 2 & 0 \\ 0 & 0 & 0 & 0 \end{pmatrix} H^v_{(s_1,t_1)}(f)^T = 0$$

Then,

$$\frac{\partial f(v)}{\partial s_1} = 0, \ \frac{\partial f(v)}{\partial t_1} = 0;$$

3. *When* $n \mod 4 = 3$*, the Hermite data should satisfy*

$$H^v_{(s_1,t_1)}(f)^T = A_1 H^v_{(s_1,t_1)}(f)^T,$$

i.e.

$$\begin{pmatrix} 0 & 0 & 0 & 0 \\ 0 & 1 & -1 & 0 \\ 0 & 1 & 1 & 0 \\ 0 & 0 & 0 & 2 \end{pmatrix} H^v_{(s_1,t_1)}(f)^T = 0$$

Then,

$$\frac{\partial f(v)}{\partial s_1} = 0, \ \frac{\partial f(v)}{\partial t_1} = 0, \ \frac{\partial^2 f(v)}{\partial s_1 \partial t_1} = 0.$$

Proof. We just expressed the C^1 fit along each edge shared by adjacent cells. □

We recall that, by Definition 2.3, a hanging vertex v is a non end vertex of a composite edge, which belongs to the interior of a segment joining two corner points of a cell. For hanging vertices, similar to Theorem 4.2 in [17], we get

Lemma 3.7. *Let $v_0, v_1, \ldots, v_\ell$ be all vertices on a composite edge of $\mathscr{M}$ and $f \in \mathbf{S}(3,1;\mathscr{M})$. Then the Hermite data $H^{v_i}(f)$ depends linearly on $H^{v_0}(f)$ and $H^{v_\ell}(f)$, where v_i is a hanging vertex , for $i = 1, 2, \ldots, \ell - 1$.*

Moreover, a hierarchical parametric mesh is T-cycle free. For a T-cycle free mesh, the Hermite data at a hanging vertex can be decided by the Hermite data at basis vertices, as [18].

Let $\mathscr{M}$ be a hierarchical mesh. The results of Sections 3.1.1, and 3.1.2 imply the following proposition.

Proposition 3.8. *The map $\mathscr{H}$ defined in* (3) *can be reduced to*

$$\begin{aligned}\widetilde{\mathscr{H}} :&\mathbf{S}(3,1;\mathscr{M}) \to \mathbb{R}^{4N_1+2N_2+N_3},\\ &f \mapsto \oplus_{v\in V}\widetilde{H}^v(f)\end{aligned}$$

where V is the set of basis vertices of $\mathscr{M}$ and

- $\widetilde{H}^v(f) = H^v(f)$, *if v is a boundary vertex or* $\deg(v) \mod 4 = 0$,
- $\widetilde{H}^v(f) = [f(v), \frac{\partial^2 f(v)}{\partial s \partial t}]$, *if* $\deg(v) \mod 4 = 2$,
- $\widetilde{H}^v(f) = [f(v)]$, *if* $\deg(v) \mod 2 = 1$.

Here, N_1 is the number of boundary vertices and interior basis vertices with $\deg(v) \mod 4 = 0$, *N_2 is the number of interior basis vertices with* $\deg(v) \mod 4 = 2$, *and N_3 is the number of interior basis vertices with* $\deg(v) \mod 2 = 1$. *$\widetilde{\mathscr{H}}$ is injective.*

Indeed, based on Lemma 3.7, if all Hermite data at the basis vertices vanish, then $H^v(f) = \mathbf{0}$ for any vertex v of $\mathscr{M}$. Thus, for any cell of $\mathscr{M}$, the Hermite data of f at any vertex of this cell is zero, i.e., $f \equiv 0$. In other words, $\widetilde{\mathscr{H}}$ is injective.

In the next section, we will construct splines associated with a basis vertex of a hierarchical parametric mesh $\mathscr{M}$ and prove that $\widetilde{\mathscr{H}}$ is surjective.

3.2. Dimension formulas and Hermite bases

In this section, $\mathscr{M}$ is a hierarchical parametric mesh obtained by a sequence of refinements:

$$\mathscr{M}^0 \longrightarrow \cdots \mathscr{M}^k \longrightarrow \cdots \longrightarrow \mathscr{M}^l = \mathscr{M}.$$

We will continue to analyze $\widetilde{\mathscr{H}}$ introduced in Proposition 3.8. By proving that $\widetilde{\mathscr{H}}$ is a surjection, the dimension formulae of $\mathbf{S}(3,1;\mathscr{M})$ are given, and the spline set constructed in Theorem 3.10 is a basis set called Hermite bases.

As we have seen (Proposition 3.8), a spline function f over $\mathscr{M}$ is uniquely determined by its Hermite data $\widetilde{\mathscr{H}}(f)$. The following lemma shows that the image of the linear map $\widetilde{\mathscr{H}}$ is the vector space of Hermite data that are compatible across each edge of $\mathscr{M}$.

Lemma 3.9. *If the Hermite data at the vertices of the cells $C_1, \ldots, C_N$ are compatible, there exists a unique element $f \in \mathbf{S}(3,1;\mathscr{M})$ with this Hermite data.*

Proof. Let us consider two vertices v_1, v_2 of a common edge between two cells C_{i_1}, C_{i_2} of $\mathscr{M}$. We can assume that the transition map is the identity map. Let f_1 (resp. f_2) be the unique function constructed from the Hermite data at the vertices on C_1 (resp. C_2). By Lemma 3.3, f_1 and f_2 are C^1 across the common edge (v_1, v_2). This shows that the piecewise polynomial function f constructed on each cell $C_1, \ldots, C_N$ of $\mathscr{M}$ from the Hermite data at their vertices is in $\mathbf{S}(3,1;\mathscr{M})$. As $\widetilde{\mathscr{H}}$ is injective, the function f is uniquely determined by its Hermite data. □

In the following, we are going to construct linearly independent spline functions in $\mathbf{S}(3,1;\mathscr{M})$, which image by $\mathscr{H}$ yields a basis of the vector space of compatible Hermite data. This set of spline functions is a basis of $\mathbf{S}(3,1;\mathscr{M})$.

To construct this basis, we proceed as follows. We will associate $J = 1, 2$ or 4 splines f_v^j with each basis vertex v of $\mathscr{M}$; the choice of J follows a rule described in the theorem below. We do not associate splines with hanging vertices.

Theorem 3.10. *Let v be any basis vertex of a hierarchical parametric mesh $\mathscr{M}$. We can associate with v a family of J splines f_v^j, $j = 1 \ldots J$, (J is indicated below), such that the Hermite data of each f_v^j, $j = 1 \ldots J$ at all other basis vertices $w \neq v$ of $\mathscr{M}$ are 0. While J and the Hermite data of each f_v^j, $j = 1 \ldots J$ at v are as follows.*

1. *If v is a boundary vertex or an interior vertex with $\deg(v) \mod 4 = 0$, then $J = 4$ and the Hermite data can be set equal to any one of the following choices:*

$$[1,0,0,0], [0,1,0,0], [0,0,1,0], [0,0,0,1].$$

2. *If v is an interior vertex and $\deg(v) \mod 2 = 1, 3$, then $J = 1$, and the Hermite data can be set equal to $[1,0,0,0]$.*
3. *If v is an interior vertex and $\deg(v) \mod 4 = 2$, then $J = 2$ and the Hermite data can be set equal to any one of the following choices:*

$$[1,0,0,0], [0,0,0,1].$$

Proof.
Let us first compute the Hermite data for all of the vertices of the cells of $\mathscr{M}$.
1. Set the Hermite data for all basis vertices $w \neq v$ to zero. They naturally satisfy the constraints described in Section 3.1. Thus they are compatible.
2. Set the Hermite data at v to any of the vectors mentioned in this theorem. By the constraint analysis of Section 3.1, they satisfy the compatibility condition.
3. For the Hermite data at a hanging vertex, they can be decided by the Hermite data at basis vertices of $\mathscr{M}$ as analysing after Lemma 3.7.

By Lemma 3.9, there exists a unique element of $\mathbf{S}(3,1;\mathscr{M})$ corresponding to these Hermite data. It satisfies the requirement of this theorem. □

A direct consequence of this result is the following:

Corollary 3.11. *$\widetilde{\mathscr{H}}$ is surjective.*

We deduce the dimension formula for $\mathbf{S}(3,1;\mathscr{M})$.

Theorem 3.12 (Dimension formula). *Let $\mathscr{M}$ be a hierarchical parametric mesh.*

$$\dim \mathbf{S}(3,1;\mathscr{M}) = 4N_1 + 2N_2 + N_3,$$

where N_1 is the number of boundary vertices and interior basis vertices with $\deg(v) \mod 4 = 0$*, N_2 is the number of interior basis vertices with* $\deg(v) \mod 4 = 2$*, and N_3 is the number of interior basis vertices with* $\deg(v) \mod 4 = 1, 3$*.*

Remark 3.13. *For $\mathbf{S}(d,r,\mathscr{M})$, we can analyse its dimension formula with the same method presented for $\mathbf{S}(3,1,\mathscr{M})$, where $d = 2r+1$.*

Using the functions defined by Theorem 3.10, we get a set of bases of $\mathbf{S}(3,1;\mathscr{M})$ called the **Hermite bases** of $\mathbf{S}(3,1;\mathscr{M})$. In particular, we have the following property:

Corollary 3.14 (Local Support). *Assume that $\mathscr{M}$ has no hanging vertices. Let $f_{v_i}^1, f_{v_i}^2, \ldots, f_{v_i}^{n_i}$ be all of the splines associated with the vertex v_i. Then, the support of each $f_{v_i}^j$ is within the 1-neighborhood of v_i.*

Proof. If the mesh has no hanging vertices, the Hermite data of the basis functions in Theorem 3.10 associated with a vertex v vanish at all other vertices $w \neq v$. Thus, their supports are in the union of cells of $\mathscr{M}$ containing v. □

Remark 3.15. *In [19], authors construct a G^1 surface, which is a map from a parametric domain to $\mathbb{R}^3$, over a parametric mesh for applications in geometric modelling. In this paper, we construct spline functions over a parametric mesh and take them as shape functions, trial functions and test functions for numerical analysis. To validate analysis properties of these spline functions for solving the Grad-Shafranov equation, H^1 integrability assumption of parameterizations will be discussed in the next section.*

4. Convergence behavior with bicubic Hermite bases

In this section, we analyze the practicability of the splines defined in this paper. Based on the steps of solving the target application in the Introduction, two aspects should be considered. The first is generating a parameterization represented by the Hermite bases constructed in Section 3.2. A sketch of the algorithm is given in Section 4.1. Further works of generating parameterizations will be presented elsewhere. By this algorithm, we analysis the property of parameterization for solving the Grad-Shafanov equation. The second is the convergence behavior of solving PDEs by taking these Hermite bases as shape functions, test functions and trial functions. This will be discussed in Section 4.2.

4.1. Parameterization

There are three steps for generating a parameterization σ that aligns curves called iso-curves.

- Based on the iso-curves, design a parametric mesh $\mathscr{M}$ such that these iso-curves can be treated as the image of some mesh grid lines of $\mathscr{M}$ under a parameterization;
- Choose positions $\mathbf{Q} = \{Q_i\}$ on the physical domain and their parameters $\mathbf{P} = \{P_i\}$ with frame $\mathscr{F}$, where we expect $\sigma(P_i) = Q_i$;
- Minimize the energy E:

$$E = \sum_{P_i \in \mathbf{P}} \omega_i ||\sigma(P_i) - Q_i||^2, \tag{9}$$

  where $\{\omega_i\}$ are weights.

Then, a parameterization $\sigma : \mathscr{M} \longrightarrow \Omega$ is obtained, where Ω is a physical domain. The choice of weights follows a rule implying that the iso-curves in the physical domain can be aligned by mesh grid lines.

The following is an example. In this example, the topology of the parametric mesh is the same as that of the mesh of the target application.

Example 4.1.

The physical domain Ω shown in the left of Figure 8 is bounded by $y^2 - x(x-1)^2 = 2, (x-2)^2 + y^2 = 0.25, x = 2, (x-0.5)^2 + y^2 = (\sqrt{2}/10)^2$. The iso-curves are given by $F0 : y^2 - x(x-1)^2 = 0$, $F2 : y^2 - x(x-1)^2 = 2$, $X2 : x = 2$, $C0 : (x-0.5)^2 + y^2 = (\sqrt{2}/10)^2$ and $C1 : (x-2)^2 + y^2 = 0.25$. Then we construct a parametric mesh $\mathscr{M}$ shown in the left of Figure 7. Some grid lines of $\mathscr{M}$ are expected to align the iso-curves shown on the right of Figure 7.

Take $\mathbf{Q} = \{Q_i\}$ in Ω and $\mathbf{P} = \{P_i\}$ on $\mathscr{M}$, where $\mathbf{Q}$ is shown in the middle of Figure 8. Then, minimize the energy (9) with weights of 1.5 for the points on the iso-curves and weights of 1.0 for the other points. The obtained parameterization σ is obtained shown on the right of Figure 8.

- Based on Example 4.1, Hermite bases can be used to represent the physical domain with complex iso-curves. However, even if there are 4 degree of freedoms at v_0 in Figure 7, there is only one freedom used by the result of this algorithm. Thus, there is a singularity at v_0, i.e., the Jacobian of this parameterization at v_0 is zero.
- To avoid a foldover, the singularities of parameterization are required at all of the interior non-hanging vertices that do not possess valence 4 (interior extraordinary vertices). In order to test a general convergence behavior of solving PDEs, in the following examples, parameterizations with singularities are chosen.

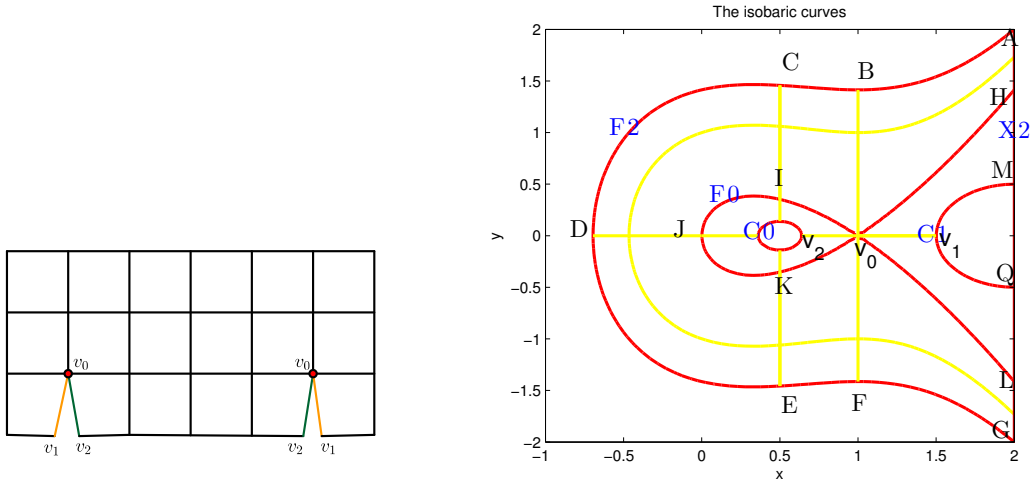

Figure 7: Parametric mesh of Example 4.1, where $\deg v_0 = 8$

- Singularities of parameterizations may introduce some problems, e.g., the required integrability assumptions for H^1 regularity properties [20] and H^2 regularity properties [21]. In the following examples for testing convergence behavior, parameterizations of physical domains are designed such that they satisfy the H^1 integrability assumptions in [20]. Because the Grad-Shafanov equation is the second order PDE.

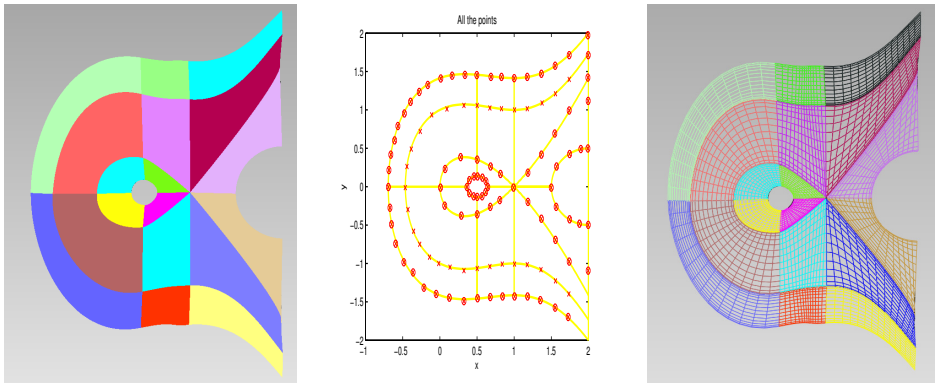

Figure 8: Physical domain (left), $\mathbf{Q} = \{Q_i\}$ (middle) and parameterization of the physical domain(right)

4.2. Convergence behavior of solving PDEs

Usually, based on the classical FEM error analysis (Theorem 6.2.1 and Proposition 6.2.2 in [22]), if the exact solution $u \in H^4(\Omega)$, error orders with L^2-norm as 4 and with H^1-norm as 3 are expected when we use bicubic splines as trial functions. In this section, the Hermite bases constructed in Section 3.2 are used to represent the

parameterizations of physical domains, and they are treated as trail and test functions when solving the model PDE. To analyse the convergence behavior of Hermite bases, its approximation error with L^2-norm is analysed. Then, several numerical examples are presented. For the target application, continuous gradients are expected. Thus, errors are measured for the examples in Section 4.2 with the H^1-norm.

Let $\mathscr{M}_0$ be an initial parametric mesh. When we subdivide its cells into 4 sub-cells, the extraordinary vertices will be surrounded by the vertices whose valences are 4, and the number of extraordinary vertices will not change. For example, the topology of the initial parametric mesh is shown on the left side of Figure 9. By subdividing, the topology of the parametric mesh is shown on the right side of Figure 9. The number of extraordinary vertices does not change, and the number of cells with an extraordinary vertex as a corner vertex does not change. Let v be an extraordinary

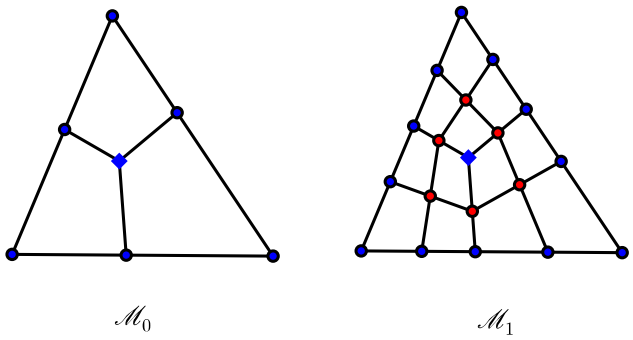

Figure 9: Subdivide the initial parametric mesh $\mathscr{M}_0$

vertex of the initial parametric mesh $\mathscr{M}_0$. After subdividing k times, parametric mesh $\mathscr{M}_k$ is obtained. There are two classes of cells of $\mathscr{M}_k$. The first is a cell with 4 regular vertices, i.e., all of the vertices are boundary vertices, or their valences are 4, the second is a cell with one extraordinary vertex as its vertex.

Theorem 4.1. *Let $\phi : \mathscr{M}_k \longrightarrow \Omega$ be a parameterization (an injective map) represented by Hermite bases over $\mathscr{M}_k$ and $\Omega = \phi(\mathscr{M}_k)$. Let $F(x, y)$ be a smooth function defined over Ω such that $F \circ \phi^{-1}|_{C_i} \in C^4(C_i)$ for any cell C_i of $\mathscr{M}_k$. Then there is a $u \in \mathbf{S}(3, 1; \mathscr{M}_k)$ and,*

$$||U(x, y) - F(x, y)||_{L^2} \leq Kh^4,$$

where K is a const, $U(x, y) = u \circ \phi^{-1}$.

Proof. First, we construct $u \in \mathbf{S}(3, 1; \mathscr{M}_k)$. For each vertex v_i of $\mathscr{M}_k$, $F \circ \phi$'s Hermite data can be used to recover a spline defined over $\mathscr{M}_k$. To be specific, let $C = [s_1, s_2] \times [t_1, t_2]$ be a cell with v_i as its vertex.

- If v_i's valence is 4 or v_i is a boundary vertex, i.e. v_i is regular, the coefficients of the 4 Hermite bases can be obtained by

$$[F \circ \phi|_C(v_i), \frac{\partial F \circ \phi|_C}{\partial s}(v_i), \frac{\partial F \circ \phi|_C}{\partial t}(v_i), \frac{\partial^2 F \circ \phi|_C}{\partial s \partial t}(v_i)],$$

  where (s,t) is the coordinates associated with C;

- Otherwise, the coefficients of 4 Hermite bases can be obtained by

$$[F \circ \phi(v_i), 0, 0, 0].$$

Thus, we can define a spline u over $\mathscr{M}_k$.
Now, we estimate

$$\begin{aligned} ||U(x,y) - F(x,y)||_{L^2}^2 &= \int_\Omega (U(x,y) - F(x,y))^2 dxdy \\ &= \sum_{C_i^1} \int_{\phi(C_i^1)} (U(x,y) - F(x,y))^2 dxdy + \sum_{C_i^2} \int_{\phi(C_i^2)} (U(x,y) - F(x,y))^2 dxdy \end{aligned} \tag{10}$$

where C_i^1 is a cell with 4 regular vertices and C_i^2 is a cell with one extraordinary vertex as its vertex. We will estimate $\int_{\phi(C_i^1)}(U(x,y) - F(x,y))^2 dxdy$ and $\int_{\phi(C_i^2)}(U(x,y) - F(x,y))^2 dxdy$, respectively.
Case 1: If there are 4 Hermite bases at each vertex of cell $C_i^1 = [s_1, s_1+h] \times [t_1, t_1+h]$ of $\mathscr{M}_k$, $u|_{C_i^1}$'s Hermite data at each vertex of C_i^1 is the same as the Hermite data of $F \circ \phi|_{C_i^1}$ at these vertices. Thus, by Theorem 4 in [23],

$$|F \circ \phi|_{C_i^1}(s,t) - u(s,t)| \leq K_1 h^4, \tag{11}$$

where K_1 is a const, $u(s,t) = u|_{C_i^1}(s,t)$. Thus,

$$\begin{aligned} \int_{\phi(C_i^1)} (F(x,y) - U(x,y))^2 dxdy &= \int_{C_i^1} (F \circ \phi|_{C_i^1}(s,t) - u|_{C_i^1}(s,t))^2 \mathscr{J}_{C_i^1}(s,t) dsdt \\ &\leq K_2 (h^4)^2 \int_{C_i^1} dsdt \\ &= K_2 h^{10}, \end{aligned}$$

where

$$\mathscr{J}_{C_i^1}(s,t) = \begin{vmatrix} \frac{\partial x(s,t)}{\partial t} & \frac{\partial x(s,t)}{\partial s} \\ \frac{\partial y(s,t)}{\partial s} & \frac{\partial y(s,t)}{\partial t} \end{vmatrix}$$

with $\phi|_{C_i^1}(s,t) = [x(s,t), y(s,t)]$, K_2 is a const.

Owing to the subdivision, the number of this type of cell is less than $1/h^2$ if the initial cell size of $\mathscr{M}_0$ is 1. Thus,

$$\begin{aligned}\sum_{C_i^1}\int_{\phi(C_i^1)}(U(x,y)-F(x,y))^2dxdy &\le K_2h^{10}*(1/h^2)\\ &= K_2h^8.\end{aligned} \tag{12}$$

Case 2: Let C_i^2 be a cell that takes an extraordinary vertex v as one of its vertices. Then the other three vertices v_1, v_2, v_3 of C_i^2 are the vertices with valence 4. Suppose $C_i^2 = [s_1, s_1+h]\times[t_1, t_1+h]$, $v_1(s_1,t_1), v_2(s_1+h,t_1), v_3(s_1,t_1+h), v(s_1+h,t_1+h)$. Then the spline u defined over $\mathscr{M}_k$ satisfies

- $u(v) = F\circ\phi(v)$;
- $H^{v_i}_{(s,t)}(u) = H^{v_i}_{(s,t)}(F\circ\phi)$, i. e. ,

$$\begin{aligned}&u(v_i) = F\circ\phi(v_i);\quad \frac{\partial u(v_i)}{\partial s} = \frac{\partial F\circ\phi(v_i)}{\partial s};\\ &\frac{\partial u(v_i)}{\partial t} = \frac{\partial F\circ\phi(v_i)}{\partial t};\quad \frac{\partial^2 u(v_i)}{\partial s\partial t} = \frac{\partial^2 F\circ\phi(v_i)}{\partial s\partial t},\end{aligned}$$

  where $i = 1, 2, 3$.

Denote $\psi(s,t) = F\circ\phi|_{C_i^2}(s,t) - u|_{C_i^2}(s,t)$, then,

$$\psi(v_1) = 0, \frac{\partial\psi}{\partial s}(v_1) = 0, \frac{\partial\psi}{\partial t}(v_1) = 0.$$

By Taylor expansion at v_1, there is $v_p \in C_i^2$ such that

$$\psi(s,t) = \frac{1}{2!}\frac{\partial^2\psi}{\partial\mathbf{l}^2}(v_p)(s-s_0)(t-t_0),$$

where $\mathbf{l} = v_p\vec{v}_1/|v_p\vec{v}_1|$. There is a const C such that

$$|\frac{\partial^2\psi}{\partial\mathbf{l}^2}(v_p)| \le C$$

when $\psi(s,t)\in C^4$. Thus, there is a const K_3 such that

$$|F\circ\phi|_{C_i^2}(s,t) - u|_{C_i^2}(s,t)| \le K_3h^2. \tag{13}$$

Suppose $\phi|_{C_i^2}(s,t) = [x(s,t), y(s,t)]$. Then,

$$\begin{aligned}&\frac{\partial x(v)}{\partial s} = 0,\quad \frac{\partial x(v)}{\partial t} = 0;\\ &\frac{\partial y(v)}{\partial s} = 0,\quad \frac{\partial y(v)}{\partial t} = 0.\end{aligned}$$

By Taylor expansion the Jacobian of ϕ over C_i^2 is

$$\mathscr{J}_{C_i^2}(s,t) = \begin{vmatrix} \frac{\partial x(s,t)}{\partial t} & \frac{\partial x(s,t)}{\partial s} \\ \frac{\partial y(s,t)}{\partial s} & \frac{\partial y(s,t)}{\partial t} \end{vmatrix} \sim h^2.$$

Thus there is a const K_4 such that

$$\begin{aligned}\int_{\phi(C_i^2)} (U(x,y) - F(x,y))^2 dxdy =& \int_{C_i^2} (F\circ\phi|_{C_i^2}(s,t) - u|_{C_i^2}(s,t))^2 \mathscr{J}_{C_i^2}(s,t) dsdt \\ \leq& K_4 h^6 \int_{C_i^2} dsdt \\ =& K_4 h^8.\end{aligned}$$

Owing to the subdivision, the number of the second type of cells does not change, i.e., it is a const for each $\mathscr{M}_k$. Thus, there is a const K_5 such that

$$\sum_{C_i^2} \int_{\phi(C_i^2)} (U(x,y) - F(x,y))^2 dxdy \leq K_5 h^8. \tag{14}$$

Based on (12) and (14), there is a const K_6 such that

$$\begin{aligned}E^2 =& \int_\Omega (U(x,y) - F(x,y))^2 dxdy \\ =& \sum_{C_i^1} \int_{\phi(C_i^1)} (U(x,y) - F(x,y))^2 dxdy + \sum_{C_i^2} \int_{\phi(C_i^2)} (U(x,y) - F(x,y))^2 dxdy \\ \leq& K_6 h^8.\end{aligned} \tag{15}$$

By (15), for $F(x,y)$ defined over Ω, there is a spline u defined over $\mathscr{M}_k$ such that

$$||U(x,y) - F(x,y)||_{L^2} = \sqrt{\int_\Omega (U(x,y) - F(x,y))^2 dxdy} \leq K h^4,$$

where $U(x,y) = u \circ \phi^{-1}(x,y)$, K is a const. In other words, for a smooth function $F(x,y)$ defined over the physical domain, there is a spline u defined over $\mathscr{M}_k$ that can be used to approximate $F(x,y)$ by an injective parameterization ϕ with an error order of 4. □

In the following, some examples are presented to test the error order caused by spline space in this paper. The reasons for choosing these examples are the following. 1. The physical domain can be exactly described by the parameterization with Hermite bases. The error between the exact solution and the solution given by the isoparametric finite element method or isogeometric analysis comes from two parts. One is the approximation error of the trail functions. The other is the approximation error of the physical domain by the shape functions. Thus, to test the error orders that come from

the approximation of our spline spaces of solving PDEs, we choose physical domains that can be exactly described by Hermite bases.

2. The Grad-Shafanov equation [24] is chosen as the model PDE problem. Let Ω be a physical domain. The generic form of the fixed-boundary Grad-Shafranov equation can be written as

$$\begin{aligned} &\triangle^* u = f_0(u, x, y) \ \text{ in } \ \Omega \\ &u = 0 \ \text{ on } \ \partial\Omega \end{aligned} \tag{16}$$

where

$$\begin{aligned} \triangle^* u =& x\frac{\partial}{\partial x}\left(\frac{1}{x}\frac{\partial u}{\partial x}\right) + \frac{\partial^2 u}{\partial y^2} \\ =& x\nabla(X\nabla u), \end{aligned}$$

and

$$X = \begin{pmatrix} 1/x & 0 \\ 0 & 1/x \end{pmatrix}$$

Thus, in the following examples, we consider

$$\begin{aligned} -\nabla(R(x)\nabla u) = -r(x)f(u, x, y) \ \text{ in } \ \Omega, \\ u = 0 \ \text{ on } \ \partial\Omega, \end{aligned} \tag{17}$$

where $r(x)$ is a function of x and

$$R(x) = \begin{pmatrix} r(x) & 0 \\ 0 & r(x) \end{pmatrix}.$$

Case 1. If $f(u, x, y) = f(x, y)$, i.e., $f(u, x, y)$ has no relationship with u, then the weak form of this model PDE (17) can be stated as follows. Given f, find $u \in V$, such that for all $v \in V$,

$$a(u, v) = l(v), \tag{18}$$

where $V = \{v : v \in \mathbf{H}^1(\Omega), v|_{\partial\Omega} = 0\}$, $\mathbf{H}^1(\Omega)$ is the Sobolev space that consists of the functions in $\mathbf{L}^2(\Omega)$ that possess weak and square-integrable derivatives. $a(u, v)$ is the symmetric bilinear form defined as

$$a(u, v) = \int_\Omega \nabla u R(x) \nabla v^T \mathrm{d}\Omega,$$

$l(v)$ is a linear functional defined as

$$l(v) = -\int_\Omega r(x) f(x, y)\, v \,\mathrm{d}\Omega.$$

We discretize the weak form, Eq. (18), with our splines. The linear system

$$\mathbf{Ad} = \mathbf{F} \tag{19}$$

is obtained, where $\mathbf{A}$ is the stiffness matrix, $\mathbf{F}$ is the force vector and $\mathbf{d}$ is the displacement vector.

Case 2. For a general $f(u, x, y)$ such that (17) is a nonlinear Grad-Shafranov equation, the Picard iteration method is used to compute the solution. Take $u_0(x, y)$ as an initial solution. Suppose that the $i-$th iteration solution $u_i(x, y)$ has been obtained. Solve the $(i + 1)-$th iteration solution $u_{i+1}(x, y)$ with

$$\begin{aligned} -\nabla(R(x)\nabla u_{i+1}(x, y)) &= -r(x)f(u_i(x, y), x, y) \ \text{ in } \ \Omega, \\ u_{i+1} &= 0 \ \text{ on } \ \partial\Omega, \end{aligned}$$

by the method presented in Case 1. Then the solution of model PDE (17) is given by

$$u(x, y) = \lim_{i\to\infty} u_i(x, y)$$

3. Generally, there are singularities of parameterizations at extraordinary vertices. By subdividing parameter meshes, these extraordinary vertices are surrounded regular vertices, i.e. they are isolated. Suppose that extraordinary vertices of the initial parameter meshes of these examples are isolated. And the initial parameterizations are satisfy Assumption 5.1 in [20] with $\alpha = (2, 2)$ and $\mathbf{p} = (3, 3)$.

If we represent a parameterization with the combination of Bezier polynomials on each cells with one extraordinary vertex $\mathbf{O}$, denoted as $\sigma(s, t)$, the positions of control points refered to Assumption 5.1 in [20] are determined by $\frac{\partial^2\sigma}{\partial s^2}|_{\mathbf{O}}, \frac{\partial^2\sigma}{\partial t^2}|_{\mathbf{O}}$, $\frac{\partial^3\sigma}{\partial s^2\partial t}|_{\mathbf{O}}$ and $\frac{\partial^3\sigma}{\partial s\partial t^2}|_{\mathbf{O}}$. Thus, during the subdivision, σ satisfies Assumption 5.1 in [20] over the finer parameter mesh if σ satisfies this integrability assumption over the initial parameter mesh. In the following examples, during the subdivision of parameter meshes, the parameterizations don't change and the initial parameterzations satisfy Assumption 5.1 in [20].

There are two examples. All of the physical domains of these examples can be exactly described by Hermite bases. Thus, the errors come from approximation by Hermite bases. In Example 4.2, we take $r(x) \equiv 1$ and $f(u, x, y) = f(x, y)$ in the model PDE (17). In Example 4.3, $r(x) = 1/(x + 2)^2$ and $f(u, x, y) = f(x, y) + u^2$, where $f(x, y)$ will be defined in Example 4.3.

Example 4.2.

1. The physical domain is shown on the left side of Figure 10, and its boundary is composed of the solutions of nine implicit bicubic polynomials, i. e., there are $F_1(x, y), F_2(x, y), \cdots, F_9(x, y)$ which are bicubic polynomials, such that the boundary

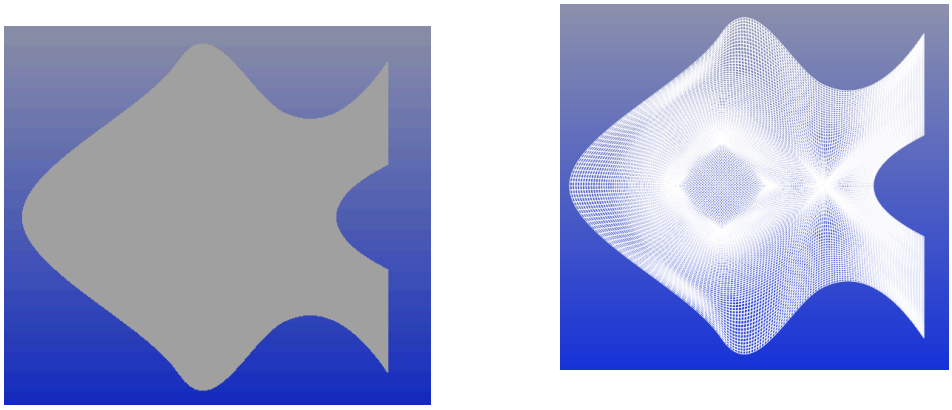

Figure 10: The physical domain and the parameterization of Example 4.2

of this physical domain is a part of the solution of the following system:

$$\begin{cases} F_1(x,y) = 0 \\ F_2(x,y) = 0 \\ \cdots\cdots \\ F_9(x,y) = 0 \end{cases}$$

2. The initial parametric mesh has the same topology as the "usual" mesh shown in Figure 11.

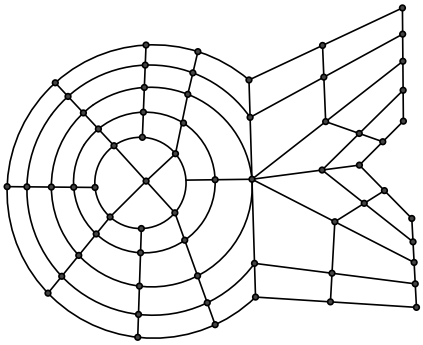

Figure 11: The "usual" mesh that has the same topology as the initial parametric mesh of Example 4.2

3. Take $r(x) \equiv 1$, and taking the exact solution of the model PDE (17) as $u = (x+2)(x+1)\Pi_i^9 F_i(x,y)/10000$. Then, the right side term is $f(x,y) = -\Delta u$, i. e., the PDE is

$$\begin{aligned} -\Delta u &= f \quad \text{in} \quad \Omega; \\ u &= 0 \quad \text{on} \quad \partial\Omega. \end{aligned}$$

Moreover, the initial parameterization of the physical domain is shown on the right side of Figure 10 with the exact boundary representation of the physical domain;

We globally refine the spline space by recursively splitting each of the original cells of the mesh into four subcells. In Figure 12, there are errors measured by L^2-norm and H^1-norm.

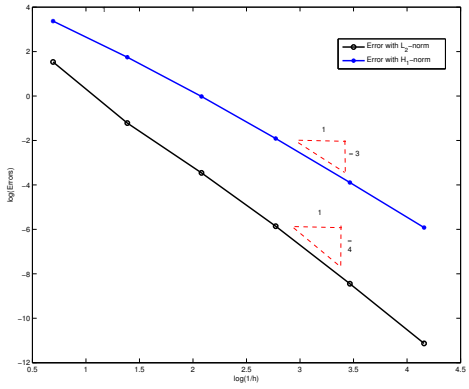

Figure 12: Errors with the L^2-norm and H^1-norm

Example 4.3.

1. The physical domain is the square $\Omega = [-1, 1] \times [-1, 1] \subset \mathbb{R}^2$;
2. We take $r(x) = 1/(x+2)^2$ $f(u, x, y) = g(x, y) + u^2$ so that the exact solution of the model PDE (17) is $u = (1 - x^2)(1 - y^2)$, where $g(x, y) = -(1 - x^2)^2(1 - y^2)^2 + 2(1 - y^2) - 8(1 - y^2)/(x + 2) - 2(1 - x^2)$. Under these conditions, the PDE is

$$-(x+2)^2\nabla(R(x)\nabla u) = -g(x,y) - u^2 \quad \text{in} \quad \Omega,$$
$$u = 0 \quad \text{on} \quad \partial\Omega,$$

where $r(x)$ is a function of x and

$$R(x) = \begin{pmatrix} 1/(x+2)^2 & 0 \\ 0 & 1/(x+2)^2 \end{pmatrix}.$$

3.The initial parametric mesh has the same topology as the "usual" mesh shown in Figure 13;
4. The parameterization of Ω (with an exact boundary representation) is described in Figure 14.

We globally refine the spline space by recursively splitting each of the 8 cells of the mesh into four subcells. In Figure 15, there are errors measured by L^2-norm and H^1-norm.

For Examples 4.2 and 4.3, the error order with L^2-norm is approximately 4 and that with H^1-norm is approximately 3. That means, by these numerical examples, the optimal error orders are reached.

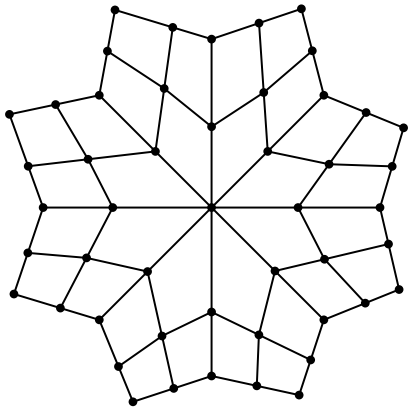

Figure 13: The "usual" mesh that has the same topology as the initial parametric mesh of Example 4.3

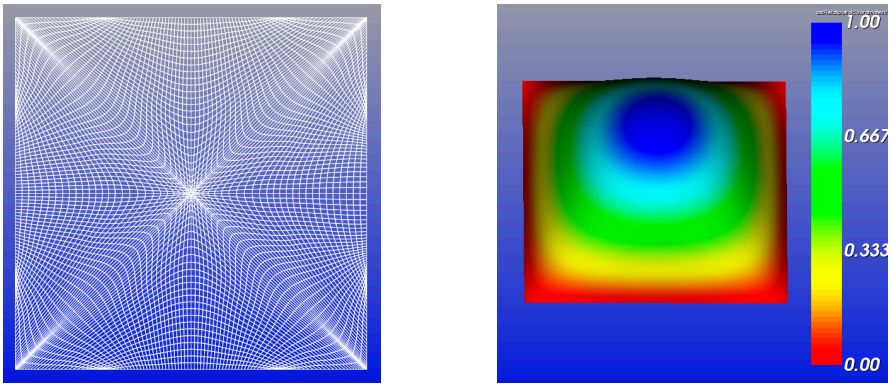

Figure 14: The parameterization of Ω and the isoparametric solution

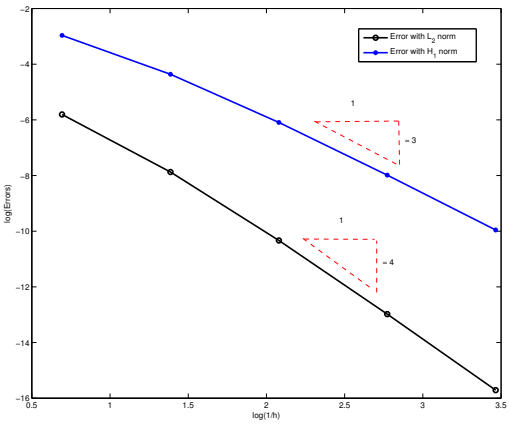

Figure 15: Errors with the L^2-norm and H^1-norm

5. Conclusion and future work

This paper presents the definition of spline spaces over rectangular meshes with arbitrary topologies. A rule for local refinement of parametric meshes is presented, and the changes in spline space over these refined parametric meshes were studied by taking transition maps as rigid transformations. Moreover, for bi-cubic spline spaces with C^1 continuity, the dimension formulae are given. Its basis functions, called Hermite bases, are also constructed.

With the help of Hermite bases, the practicability of these splines for solving the Grad-Shafranov equation is analyzed. Generally, isolated singularities of parameterizations may be involved. For solving the Grad-Shafranov equation, the parameterizations are satisfied H^1 integrability assumptions in [20]. Based on the results of examples, the optimal error orders with L^2-norm and H^1-norm are reached.

For a better solution of the MHD simulation over a general physical domain, in the futher, it is necessary to develop a method of generating a parameterization in the following directions:

- generating a parameterization algorithm that satisfes integrability assumptions. Here, more general transition maps or higher degree of spline spaces should be considered;
- generating a parameterization algorithm for modifying the quality of stiffness matrix;
- generating a parameterization algorithm for a better approximation of the boundaries of physical domains.

Reference

[1] O. Czarny and G. Huysmans. Bézier surfaces and finite elements for MHD simulations. *Journal of Computational Physics*, vol. 227, p. 7423–7445, 2008.

[2] I. Ergatoudis, B. Irons, and O. Zienkiewicz. Curved isoparametric "quadrilateral" elements for finite element analysis. *Int. J. Solids Structures*, vol. 4, p. 31–42, 1968.

[3] T. J. R. Hughes, J. A. Cottrell and Y. Bazilevs "Isogeometric analysis: CAD, finite elements, NURBS, exact geometry and mesh refinement". *Computer Methods in Applied Mechanics and Engineering*, vol. 194, Issues. 39-41, p. 4135–4195, 2005.

[4] K. Höllig. *Finite Element Methods with B-Splines.* SIAM, 2003.

[5] D. R. Forsey and R. H. Bartels. Hierarchical B-spline refinement. In *Proceedings of the 15th annual conference on Computer graphics and interactive techniques*, SIGGRAPH '88, pages 205–212, New York, NY, USA, 1988. ACM.

[6] R. Kraft, Adaptive and linearly independent multilevel B-splines. In Surface Fitting and Multiresolution Methods, A. L. Méhauté, C. Rabut, and L. L. Schumaker, Eds., vol. 2. Vanderbilt University Press, p. 209 – 216.

[7] C. Giannelli, B. Jüttler, and H. Speleers. THB-splines: The truncated basis for hierarchical splines. *Computer Aided Geometric Design*, 29(7):485 – 498, 2012.

[8] T. Dokken, T. Lyche, and K. Pettersen. Polynomial splines over locally refined box-partitions. *Computer Aided Geometric Design*, 30(3), p. 331–356, 2013.

[9] T. W. Sederberg, J. Zheng, A. Bakenov, A. Nasri. T-splines and T-NURCCs. *ACM Trans. Graph.*, vol. 22, p. 161–172, 2003.

[10] X. Gu, Y. He, H. Qin, Manifold splines. *Graphical Models*, vol. 68, p. 237–254, 2006.

[11] Y. He, K. Wang, H. Wang, X. Gu, H. Qin, Manifold T-spline. *Geometric Modeling and Processing-GMP 2006, Lecture Notes in Computer Science*, vol. 4077, p. 409–422, 2006.

[12] H. Wang, Y. He, X. Li, X. Gu, H. Qin, Polycube Splines. *Computer-Aided Design*, vol. 40, p. 721–733, 2008.

[13] L. Ying, D. Zorin, A simple manifold-based construction of surfaces of arbitrary smoothness. *ACM Trans. Graph.*, vol. 23, p. 271–275, 2004.

[14] J. Peter, U. Reif, Subdivision Surfaces. *Geometry and Computing, Springer-Verlag*, ISBN 878-3-540-76406-9, 2008.

[15] G. T. A. Huysmans, J. P. Goedbloed. "Isoparametric Bicubic Hermite Elements for Solution of the Grad-Shafranov Equation". *International Journal of Modern Physics C*, p. 371-376, 1991.

[16] K. H. Huebner, E. A. Thornton. The Finite Element Method for Engineers. *John Wiley & Sons*, ISBN 0-471-09159-6, 1982.

[17] J. Deng, F. Chen, and Y. Feng. Dimensions of spline spaces over T-meshes. *Journal of Computational and Applied Mathematics*, vol. 194, p. 267–283, 2006.

[18] L. L. Schumaker and L. Wang. Approximation power of polynomial splines on T-meshes *Computer Aided Geometric Design* 29, p. 599 – 612, 2012

[19] Xin Li, Jiansong Deng, Falai Chen "Polynomial splines over general T-meshes". *The Visual Computer*, vol. 26, p. 277-286, 2009.

[20] T. Takacs, B. Jüttler. "Existence of Stiffness Matrix Integrals for Singularly Parameterized Domains in Isogeometric Analysis". *Computer Methods in Applied Mechanics and Engineering*, vol. 200, p. 3568–3582, 2011.

[21] T. Takacs, B. Jüttler. "H^2 regularity properties of singular parameterzations in isogeometric analysis". *Graphical Models*, vol. 74, p. 361–372, 2012.

[22] A. Quarteroni, A. Valli. Numerical Approximation of Partial Differential Equations. *Springer-Verlag*, ISBN 3-540-57111-6, 1997.

[23] L. L. Schumaker, L. Wang. On Hermite interpolation with polynomial splines on T-meshes. *Journal of Computational and Applied Mathematics*, vol. 240, p. 42–50, 2013.

[24] A. Pataki, A. J. Cerfon, J. P. Freidberg, L. Greengard and M. O. Neil. A fast, high-order solver for the Grad-Shafranov equation. *J. Comput. Phys.*, vol. 243, p. 28–45, 2013.

[25] B. Mourrain. On the dimension of spline spaces on planar T-meshes. *Mathematics of Computation*, 83, p. 847–871, 2014.